GRAPHENE OXIDE AS A DELIVERY SYSTEM FOR OXALIPLATIN IN 2D AND 3D TUMOUR MODELS

By

XIAORAN WANG

A thesis submitted to the University of Birmingham for the degree of

MSC BY RESEARCH

The school of Pharmacy

University of Birmingham

March 2022

UNIVERSITY OF
BIRMINGHAM

University of Birmingham Research Archive

e-theses repository

This unpublished thesis/dissertation is copyright of the author and/or third parties. The intellectual property rights of the author or third parties in respect of this work are as defined by The Copyright Designs and Patents Act 1988 or as modified by any successor legislation.

Any use made of information contained in this thesis/dissertation must be in accordance with that legislation and must be properly acknowledged. Further distribution or reproduction in any format is prohibited without the permission of the copyright holder.

Abstract

Graphene oxide (GO) has attracted a lot of attention in recent years as a novel drug delivery system due to its good stability and biocompatibility. However, the understand and research of GO ability to deliver anticancer drugs inside 2D monolayer cells as well as 3D tumour models need to be further. There is a gap in this field. For instance, the complexation of GO with platinum anticancer drugs is still under-investigated. In this study, the cell viability of oxaliplatin in 2D monolayer cells was assessed on colorectal (HCT116) and breast (MCF7) cancer cells at different seeding densities (5000 & 7000 cells per well) for 24 and 48hrs.

Next, we looked at the ability of graphene oxide (GO) to deliver the anticancer drug oxaliplatin. GO was prepared using the modified Hummer's Methods and characterisation suggested the preparation of stable GO. The different concentrations of oxaliplatin were complexed with GO and assessed the cell viability on colorectal cancer cells (HCT116) and breast cancer cells (MCF7). The MTT and modified LDH assays were used to assess the cell viability of oxaliplatin alone and complexed with GO at different concentration and time points. It was found that GO complexed with oxaliplatin showed a dose-dependent trend on HCT116 cells after 48hrs but was not higher than oxaliplatin alone. In MCF7 cells, the combination therapy showed a higher reduction in cell viability especially at the highest concentration of oxaliplatin used for 48hrs.

Spheroids are an excellent 3D model to research the response of cancer cells to drugs and mimic the microenvironment of tumour *in vitro*. The establishment of an *in vitro* 3D cell culture model like

spheroids will improve our understanding of the gap between two-dimensional cell culture and animal experiments. In this work, MCF7 based spheroids were prepared using the Liquid Overlay Method and then treated with GO alone, oxaliplatin alone and GO: oxaliplatin complexes to assess the ability of GO to deliver oxaliplatin inside the spheroids. After 48hrs and 72hrs following treatment of MCF7 spheroids with the combination therapy, a slight inhibition in the spheroid growth was observed which could be explained by the effective delivery of oxaliplatin inside the spheroids. In conclusion, GO could indeed become a potential drug delivery nanocarrier especially for platinum based anticancer drugs.

Keywords

Graphene oxide; oxaliplatin; HCT116; MCF7; 3D spheroid; Drug delivery system; cytotoxicity assessment

Acknowledgements

This work was technically supported by University of Birmingham. The author gratefully acknowledges the academic support from my supervisor Dr. Hanene Ali-Boucetta and Dr. Marie-Christine Jones. Dr. Hanene Ali-Boucetta was instrumental in each stage of my process. For this, I am extremely grateful. I would like to acknowledge my research partner in my lab and acknowledge Carina and parents for their company and understanding.

List of contents

List of Figures

List of Tables

List of Abbreviations

GO: graphene oxide

PBS: phosphate buffer saline

FBS: fetal bovine serum

DMEM: Dulbecco's Modified Eagle's Medium

DMSO: dimethyl sulfoxide

MCF7 cell: Breast carcinoma cell line

HCT116: Human Colon cancer cell

MTT: 3-(4,5)-dimethylthiahiazo (-z-y1)-3,5-di-phenytetrazoliumromide

LDH: lactate dehydrogenase

STD: standard deviation

ANOVA: statistical analysis of variation

Graphene oxide as a delivery system for oxaliplatin in 2D and 3D Tumour Models

1 Introduction

Oxaliplatin is a third generation platinum anticancer drug which is normally used for testicular, colorectal and ovary cancer therapy and more efficient on breast and melanoma cancer, which has no cardiotoxicity, nephrotoxicity and mutagenicity, a few neurotoxicity and hematologic toxicity (Mathé *et al.*, 1989), (Cassidy and Misset, 2002) . Oxaliplatin shows a significant efficacy in combination therapies with other anticancer drugs, however the current clinical studies shows that oxaliplatin would cause slight hematologic toxicity and neurotoxicity (Extra *et al.*, 1998). In addition, the sensory neuropathy is an issue with oxaliplatin which strengthened in cold condition as a result from the changes in sodium channel kinetics (Eckel *et al.*, 2002). Meanwhile, the neurotoxicity is proved to be a type of cumulative and dose-dependence toxicity (Grothey, 2003). Even though this sensory neurotoxicity is reversible, which would disappear within 4-6 months in 82% patients, it is not acceptable and safe for the patient who needs large dose or long time to therapy (Extra *et al.*, 1998). Hence, it is crucial to use drug delivery system loading oxaliplatin to

enhance the efficacy and reduce side effects. Drug delivery could be defined as a process that help the transfer of drugs to specific body site where the active ingredient is absorbed in order to achieve an efficient yet safe therapeutic outcome (De Jong and Borm, 2008). In this process a drug delivery system is used which could be based on nanoparticles. Nano-based drug delivery systems such as liposomes, carbon nanotubes and graphene oxide in **Figure 1** could be loaded with multiple drugs, illustrating the wider range of applications and prospects for multi-purpose treatment of tumours and other diseases, which is of great value and significance in cancer therapy (Couvreur, 2013).

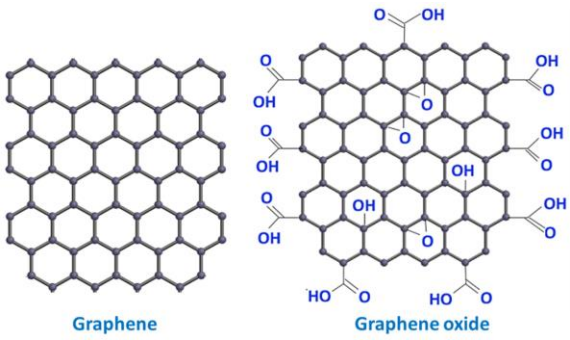

Figure 1: *Chemical structure of graphene and graphene oxide (Kausar, 2021)*

Recently, graphene and its derivatives has attracted a lot of attention for their use in the field of drug delivery and cancer therapy. Graphene based derivatives depends on multiple methods to functionalised graphene such functional group with oxygen, halogens and hydrogen (Sturala *et al.*, 2018). It has been suggested that graphene-based

nanomaterials could have an effective ability for the loading and releasing of platinum anticancer drug, while maintaining low cytotoxicity *in vitro* (L. Wei et al., 2021). Compared to the traditional nanoparticles used in drug delivery, graphene and its derivatives have excellent optical properties, large surface area and lower cost of preparation in medical area (Sun *et al.*, 2008). This research is focused on one type of graphene based nanomaterials known as graphene oxide (GO). The Nobel Prize in Physics in 2010 was awarded to Geim and his team for the discovery of graphene, a planar sheet-shape carbon nanomaterial, which has hexagonal graphite lattice consisting of bonded carbon atoms as shown in **Figure 1** (Sengupta *et al.*, 2011). Graphene oxide is the product of the oxidation of graphite, thus graphene oxide gains different characters compared to other graphene derivatives, especially in terms of improvement in its aqueous dispersion, binding site and biocompatibility (Table 1) (Borandeh *et al.*, 2021), (Abdelhalim *et al.*, 2022). Since GO has been suggested as novel drug delivery system, its safety needs to be determined. Moreover, timely drug release, accumulation in the healthy tissues and ability of tumour penetration should be considered the design of effective drug delivery system (Gu *et al.*, 2019). Therefore, there is an urgent need for comprehensive studies and research on the biocompatibility, biosafety

and degradability of graphene oxide (Mo and Gu, 2016). Various factors might influence GO cytotoxicity, for example, incubation time of GO treatment, GO concentration, cancer cells source and the type of cell model (Zuchowska *et al.*, 2020). Functionalized GO have shown a great compatibility and low cytotoxicity (L. Wei et al., 2021a). In 2013, Miao *et al.* has reported that hyaluronyl reduced graphene oxide (rGO) nanosheets have better performance on drug loading, stability, safety and anticancer effects than rGO alone (Miao *et al.*, 2013). In addition, camptothecin (CPT) could be released from PDEA-grafted GO in specific pH value which tends to be nearly acidic microenvironment as the tomour microenvironment but GO-PDEA did not have cytotoxicity for mouse neuroblastoma N2a cancer cells only when it was complexed with camptothecin (CPT). The complexes caused highly inhibition on cancer cells (Kavitha, Abdi and Park, 2013). In addition, functionalised with colloidal and human serum albumin -Nanosheets showed the less cytotoxicity but better performance of drug loading and entrapment efficiency than GO-NSs (Farnaz *et al*., 2018). Moreover, functionalised with poly (N-vinylcaprolactam) and poly (glycolic acid)-GO nanocarriers were non-toxic and highly effective towards spheroid under a pH and thermo sensitive formulation (Kazempour *et al*., 2019). The GO are more likely to functionalise for reducing the cytotoxicity

effects and avoiding the direct outcome on the cell. While Wang *et al.* found that the cytotoxicity and genetoxicity of GO assessed on human lung fibroblast (HLF) was concentration and surface charge dependent (Wang *et al.*, 2013). Moreover, Shao *et al.* showed that the cell viability of HeLa cells reduced to 80% after it was exposed under the most concentration of GO or rGO within 24h while mesoporous silica coated polydopamine reduced graphene oxide (pRGO@MS-HA) has less toxicity than GO, meanwhile, pRGO@MS-HA gain good stability and highly targeted effect in anticancer therapy (Shao *et al.*, 2017). It was also suggested that the dose and size of GO can lead to an oxidative stress in A549 lung cancer cells and the cell viability would reduce at high concentrations (up to 100 μg/ml) (Chang *et al.*, 2011). Not only the dose but also the incubation time could also impact the toxicity of GO. In carbon nanomaterial family, it is suggested that the cell uptake ratio is minimal after exposing to GO, moreover, dose-dependence and time-dependence cytotoxicity also observed after exposing to GO (Zhang *et al.*, 2012). Different studies have also suggested the potential of GO as a drug delivery system to deliver anticancer drugs. Barahuie *et al*. have illustrated that graphene oxide as a nanocarrier increased the ability of drug entrapment and anticancer efficacy with chlorogenic acid (Barahuie *et al.*, 2017). Hyaluronyl-modified rGO nanoparticles could

improve the cell uptake of doxorubicin, its good performance on stability, drugs loading and anticancer therapy effects as a potential nanoparticle for further biomedicine field (Miao *et al.*, 2013). Additionally, due to the sustained formulation properties of GO, functionalised with CuO (CuO-GO) have high toxicity and photocatalytic activity on cancer cells for targeted therapy (Ganesan *et al.*, 2020). Functionalised GO might be a tendency for reducing the GO cytotoxicity to minimal level as anticancer drug delivery nanocarriers in future studies. Therefore, GO as a novel drug delivery nanocarrier has high potential and ability for the delivery of therapeutics especially anticancer drugs in biomedicine application.

Table 1: *The characteristics and efficiencies of the GO and functionalized GO described in this article.*

GO type	Drug	Specific release factors	Mechanism (if any)	Result of safety experiments	Efficiency as drug delivery system	REFERENCE
Hyaluronyl-modified rGO nanosheets	Doxorubicin	—	Improve the drug uptake of Dox by CD-44 overexpressing	CHA-rGO has more safety, stability than rGO	Good performance on drug loading and anticancer effects	Miao, W. *et al.* (2013), *Biomaterials*, 34(37), pp. 9638–9647..2013.08.058.
PDEA-grafted GO	camptothecin	pH sensitive	——	GO -PDEA did not show the toxicity on N2a cancer cells but GO-PDET-CPT killed the cancer cell obviously.	Good stability and release the drugs at targeted site	Kavitha, T., Abdi, S.I.H. and Park, S.-Y. (2013), *Physical Chemistry Chemical Physics*, 15(14), pp. 5176–5185.
Colloidal human serum albumin	Oxaliplatin	—	Biocompatible, large surface area	Lower cytotoxicity (65%) than GO-NSs	Improve drug entrapment ratio and the ability of loading	Farnaz, R. *et al.* (2018) ,*Colloids and Surfaces B: Biointerfaces*, 171, pp. 10–16.
Folic acid (FA) molecules Sulfonic acid groups	Camptothecin; Doxorubicin	—	—	Higher cytotoxicity in dual drug using graphene oxide	Good therapy efficacy and wide application in anticancer field	Zhang, X. *et al.* (2012), *Toxicology Research*, 1(1), pp. 62–68.
Poly(N-vinylcaprolactam) ; Poly (glycolic acid)	Oxaliplatin	pH; thermo-	—	GO-PNVCL-PGA: nontoxicity; GO-PNVCL-PGA-OX: impact to cancer cells	Release drug in specific condition and good for using as a drug delivery nanoparticle	Kazempour, M. *et al.* (2019), *Journal of Drug Delivery Science and Technology*, 54, p. 101158.

Reduced GO; TAPE enzyme	silver	—	—	Good stability and efficacy of anticancer cells	Better inhibition of cancer as complex nanoparticles and high therapy efficacy	Gurunathan *et al., 2015), International Journal of Nanomedicine*, 10 (6257-6276).
3-aminopropyl triethoxysilane (APS); Fe_3O_4	Doxorubicin	pH	—	Drug release due to the pH value and assessment the cell cytotoxicity	Good performance of drug loading and targeted anticancer therapy	Yang, Z. *et al.* (2020), *ACS Omega*, 5(24), pp. 14437–14443. doi:10.1021/acsomega.0c01010.
Functionalized GO	hypocrellin A	—	Changes form of cell and nuclear	Higher stability than HA, which is a crucial index of nanoparticle	Higher drug loading efficacy, good stability and have potential as drug delivery nanoparticles	Rosli, N.F. *et al.* (2019a), *Langmuir*, 35(8), pp. 3176–3182.
CuO-	—	—	—	CuO-GO have cytotoxicity on HCT116 and reduce to 70% after exposed at 100μg/mL	High toxicity and photocatalytic response to cancer cells	Ganesan, K. *et al.* (2020), *Arabian Journal of Chemistry*, 13(8), pp. 6802–6814. 2020.06.033.
chlorogenic acid	—	pH	—	The cytotoxicity of on different cells could be negligible	High delivery ability, released and formulation properties	Barahuie, F. *et al.* (2017), *Materials Science and Engineering: C*, 74, pp. 177–185. doi:10.1016/j.msec.2016.11.114.
GO	—	—	Concentration and surface charge	GO might cause the cytotoxicity and genetoxicity of human lung fibroblast cells	Safer to modified GO in drug delivery process	Wang, A. *et al.* (2013), *Journal of applied toxicology: JAT*, 33(10), pp. 1156–1164.

mesoporous silica (MS) polydopamine hyaluronic acid (HA)-reduced graphene oxide (pRGO)	Doxorubicin	—	chemo-photothermal effect	The cytotoxicity of GO or rGO only showed around 20% toxicity at the DOX ranging most concentration. pRGO@MS-HA had reduce the toxicity to 90%	Lower cytotoxicity, good biocompatibility and targeted chemo-photothermal effect.	Shao, L. *et al.* (2017), *ACS Applied Materials & Interfaces*, 9(2), pp. 1226–1236.
GO	—	—	Dose and size dependence	A slight cytotoxicity at high GO concentration	An ideal safe nanomaterial at cellular level as the cell could grow on GO film	Chang, Y. *et al.* (2011), 200(3), pp. 201–210. doi:10.1016/j.toxlet.2010.11.016.
GO, nondiamond, MWCNTs	—	—	—	Minimal cell uptake in carbon nanoparticle family and dose-dependence toxicity	Potential application in medicine and oncology, improve the cell uptake and reduce the toxicity	Zhang, X. *et al.* (2012), *Toxicology Research*, 1(1), pp. 62–68. doi:10.1039/c2tx20006f.
Reduced graphene oxide	Ag nanoparticle	—	—	GO shows dose-dependence cytotoxicity and IC_{50} is 180μg/ml. Functionalized rGO-AgNS has cytotoxicity and IC_{50} is 30 μg/mL	Good biocompatibility and lower cytotoxicity	Kavinkumar, T. *et al.* (2017), *Journal of Colloid and Interface Science*, 505, pp. 1125–1133. 2017.07.002.
TiO2	—	visible	The phototoxicity of GOT would activate for producing ROS, reduce enzyme	The phototoxicity of GO as control group reduces around 10% cancer cells after exposed in light	Provide GO-based photosensitizers in anticancer treatment(Hu	Hu, Z. *et al.* (2012), *Carbon*, 50(3), pp. 994–1004. doi:10.1016/j.carbon.2011.10.002.

			activity	one hour.	*et al.*, 2012)	

2D monolayer cell culture has been the standard in research in cancer drug discovery for years (Kausar, 2021)(Tewari and Manetta, 1999), as they are easy to use and perform cell viability assays with them. This approach prefers to provide an easily observable and unitary environment to the cancer cells. Even though this research model has been used as a gold standard for decades, the physiological responses of 2D cancer cells differ from the real tumours microenvironment, result from abundant elements in 2D microenvironment model. For instance the difference in hypoxia/necrosis, stem cell characteristics, slow proliferation and barriers to drug diffusion (Karlsson *et al.*, 2012). Hence, the 3D cell models are significant improvement over traditional 2D model. The 3D spheroid provides a three-dimension environment for cells to grow and connect with the microenvironment, meanwhile, biological mechanisms and functionalities were promoted in cell viability, morphology, cell proliferation, gene expression, migration and invasion tissues, angiogenesis and the response to surrounding (Antoni *et al.*, 2015). Measuring the size and form of spheroid could monitor

drug cytotoxicity clearly (Baek *et al*., 2016) (Mittler *et al*., 2017). Traditional 2D monolayer cell could not reflect the tissue *in vivo* and lack of cell-to-cell or cell-to-matrix connection which could influence cell proliferation and the reaction to external factors (Abdolahinia *et al*., 2019). Moreover, the human articular chondrocytes adhesion signal and phenotype changed in monolayer model instead of 3D spheroid (Mahmood *et al*., 2014). There are different performances between cells in 3D model and monolayer model. In 2011, Bierwolf and his team found that 3D spheroid model could substantially improve the primary hepatocyte morphological changes and the activity of liver cell-specific functions, which could solve the crucial problems using 2D monolayer cells (Bierwolf *et al*., 2011). Furthermore, drug sensitivity tends to alter in 3D spheroid. The liver tumour and stromal cells in 3D spheroid model would enhance resistance to anticancer drug (Yip and Cho, 2013). Spheroid is a tissue-like microstructure, which is aggregated by cells in the media. They are cell aggregation that mimic *in vivo* tumours structurally and functionally. Several 3D culturing protocols are utilized to form spheroids. The first method is hanging drop method. This method relies on that fact the cancer cells would automatically aggregate towards the bottom of the droplet after placing drops of cell suspension on the lid of a petri dish (Del Duca, Werbowetski and Del

Maestro, 2004). This method is applied on embryonic stem cells. One of the most used method is the liquid overlay method. The cell suspension would seed on a non-adherent surface such as agar or agarose to generate spheroids rather than adhere to the bottom of the wells (Carlsson and Yuhas, 1984). Alternatively, spinner flask method (Achilli *et al.*, 2012), suspension culture techniques (Froehlich *et al.*, 2016) and centrifugation method (Handschel *et al.*, 2007) could also be used to generate a spheroid in 3D culturing. Spheroid-specific plates were also advanced, result from the high requirement of spheroid experiments, which are U-bottomed ULA plates, hanging-drop plates and nanostructured plates (Mittler *et al.*, 2017). Furthermore, a microfluidic device is used to form and treat spheroid with drug in specified spheroid size (Patra *et al.*, 2016). Dadgar et al. designed a microfluidic platform to research the responses of ovarian cancer spheroid to drugs (Dadgar *et al.*, 2020). In term of the size of spheroid, prior studies have noted the importance of microtissue size in 3D cultures which might affect the functional response of the spheroid (Asthana and Kisaalita, 2012). The type of cancer cell lines and cell density could impact the condition and the size of spheroid, hence it is necessary for each kind of cell line to be observed by prior designed assays (Sambale *et al.*, 2015). This kind of 3D model has a similar

growth microenvironment and metabolic rate *in vitro* as compared to the solid tumours *in vitro* (Costa *et al.*, 2016). Compared with 2D monolayers cell, 3D spheroids could simulate more precisely the original avascular phase and microenvironment of solid tumours (Liu *et al*., 2017). Therefore, spheroids can be used to study the effects of therapeutic agents and drug delivery system in drug development.

The aim of this work is to study and investigate the ability of GO to deliver oxaliplatin in 2D and 3D cell cultures. We hypothesis that GO will enhance the delivery of oxaliplatin in 2D monolayers and 3D spheroids.

2 Materials

Dulbecco's Modified Eagle Medium (DMEM), McCoy's 5A modified Medium, 0.25% Trypsin-EDTA (1x), fetal bovine serum (FBS), antibiotic, glutamine (stock concentration: 1%), Pen/Strep (stock concentration: 1%), agar power, DMSO (D/4120/PB08), Triton X-100 (85112, stock concentration: 10%) and LDH assay kits (C20300) were purchased from Thermo Fisher. Oxaliplatin powder, graphite powder, sodium nitrate ($NaNO_3$), sulphuric acid (H_2SO_4) (stock concentration: 98%), potassium permanganate ($KMnO_4$), 30% hydrogen peroxide and MTT power (M-5655) were purchased from Sigma-Merck Life Sciences, UK.

3 Methods

3.1 Cell culture

Breast carcinoma MCF7 cell line has been prepared in Dulbecco's Modified Eagle Medium (DMEM) completed with 10% FBS, 1% penicillin/streptomycin (stock concentration: 1%) and 1% glutamine (stock concentration: 1%). Colorectal HCT-116 cell line has been cultured in McCoy's 5A modified Medium with 10% FBS and 1%

penicillin/streptomycin. Cells were incubated and grown in humid environment at 37°C with 5% CO_2 for 3-4 days until they were confluent. Once cells proliferated to 70% confluence, they were dissociated using 0.25% Trypsin-EDTA (1x) in the incubator for 3 mins and the cell suspension was prepared in the appropriate media for the cells.

3.2 Synthesis of graphene oxide

The synthesis of graphene oxide was done according to the protocol of modified Hammers' method (Ali-Boucetta *et al.*, 2013). Firstly, 0.2g graphene powder, 0.1g sodium nitrate ($NaNO_3$) and 4.6mL sulphuric acid (H_2SO_4) (98%) were added in a conical flask which was then placed on an ice bath and stirred for 20 minutes. Secondly, 0.6g potassium permanganate ($KMnO_4$) was added slowly into the dispersion followed by the removal of the ice bath to rise the temperature to room temperature by mixing for 40 minutes. Then 9.2 mL deionized water was added dropwise, and temperature rapidly rose to around 50°C, with the aid of heating block to keep the temperature between 95 to 100°C for 45 minutes. Further dilution with 28mL warm deionized water was performed. Then 3mL hydrogen peroxide (H_2O_2) was added slowly, and the dispersion was transferred into two 50 mL

tubes. Next, warm sterile water was added to wash the dispersion and bring the pH to 7. This was performed in a biological safety cabinet to keep the GO dispersion sterile. The graphene oxide orange layer was gently collected. The sterile GO was then dried in an oven for 48hrs at 40°C.

3.3 Zeta potential of GO dispersion

The dry graphene oxide powder was resuspended in sterile water to make 30μg/mL dispersion. Typically, the GO dispersion was sonicated in an ultrasonic water bath for 15 minutes. The ZETA potential was measured using Nano-ZS (Malvern, UK). Additionally, to research the impact of difference concentration GO dispersion, the concentration of 5,10,15, 20, 30, 50, 80, 100 and 120μg/mL solution were also measured.

3.4 Ultraviolet-visible spectroscopy of GO dispersion

GO dispersions of 1, 5, 10, 20, 50μg/mL were prepared by diluting 1mg/mL GO stock solution in water. All samples were sonicated in an ultrasonic bath for 15 minutes before being scanned using UV-2600 Shimadzu, UK. Sterile water was used as the blank.

3.5 Cell Viability assessment of GO and Oxaliplatin combination

3.5.1 MTT assay

7000 cells per well were seeded in sterile 96 well plates, treated with different concentration of oxaliplatin (10-50µM) and 20% DMSO as positive control. After desired time (24 hours and 48 hours), MTT/media solution was added to each well and then incubated for around 4 hours. Afterwards, the MTT/media solution was removed and DMSO was added to solubilise the formazan crystals. The plate was read at absorbance 570nm using BMG LABTECH FLUOstar Omega (UK) microplate Reader. Negative controls were set to correct for background absorbance. The cell viability was measured using the following equation: Cell viability (%) = A (570nm of sample cells) / A (570nm of untreated cells) * 100 %.

3.5.2 Modified LDH assay

The prepared cell plates seeding 7000 cells per well were treated with oxaliplatin (10-30µM), GO (5-50µg/mL) and combination of GO and oxaliplatin at the equivalent concentration and incubated for 24hours,

48hours and 72 hours. DMSO 20% was used as a positive control. 10µL of the lysis buffer (9% Triton X-100) to 100 µL fresh media (phenol free media) was added and after one hour incubation, the cell lysate was collected and centrifuged at 13000 rpm before being transferred to a new 96 well plate. Next, reconstituted substrate mix (1 Substrate mix vial + 12 mL Assay buffer) was treated in each well and the plates were incubated for 15 minutes at room temperature. Lastly, the 50µL of Stop solution was added to each well and absorbance was read at 492nm in BMG LABTECH FLUOstar Omega (UK) microplate Reader. Negative controls were set to correct for background absorbance. The amount of LDH detected represented the number of cells which survived the treatment. The percentage cell survival was calculated using the following equation:

$$\% \text{ Cell Survival} = \frac{A_{492\text{nm of treated cells}}}{A_{492\text{nm of mean untreated cells}}} * 100\%$$

3.6 3D Spheroid formation

MCF7 and HCT116 spheroids were prepared using the liquid overlay method (Costa *et al.,* 2018). Briefly, 1% agar mixed in distilled water was autoclaved and then 100µL per well agar solution was pipetted

promptly into 96-well plate. After cooling down to room temperature, the agar solution solidified. Once MCF7 and HCT116 cells reached 70% cell confluence, cells were split, and the cell suspension was obtained. Different cell densities (from 0.5, 1, 2, 4, 8 to 10k) were prepared initially to see which cell density forms the ideal spheroids for further experiments with oxaliplatin and GO.

3.7 The effects of GO: Oxaliplatin combination on 3D spheroids

MCF7 and HCT116 spheroids were treated with GO dispersion (Concentration range 5-50 μg/ml), oxaliplatin (5-30 μM) and equivalent concentrations of GO: oxaliplatin combination for 24, 48 and 72hrs. This was initially performed directly on the agar plates but later the prepared spheroids were moved into a fresh 96 well plate to avoid any interference with the agar. In order to record the difference between the treatment groups, spheroids were imaged using optical microscopy and the size was then tabulated using ImageJ software.

3.8 Statistical analysis

Statistical analysis of MTT Assay was assessed using One-way ANOVAs and Statistical significance of mLDH Assay and 3D spheroid cytotoxicity experiment were evaluated via Two-way ANOVAs. All data are described as mean ± standard deviation. And data presented is average of at least 3 independent experiments (n=3).

4 Results

4.1 Cell Viability and Cytotoxicity assessment

4.1.1 Cell Viability of Oxaliplatin in 2D monolayer cells

MCF7 monolayer cells at 5000 cells per well were treated with 10-50µM concentration range of oxaliplatin for 24hrs and 48hrs. As shown in **Figure 2A**, it only shows around 80% cell viability in MCF7 monolayers at the concentration range between 10-50µM oxaliplatin after 24hrs treatment. After 48hrs, around 50% cell viability was observed across all concentration as shown in **Figure 2B**. DMSO 20% was used as a positive control and as expected showed around 80-90% reduction in cell viability after 24 and 48hrs.

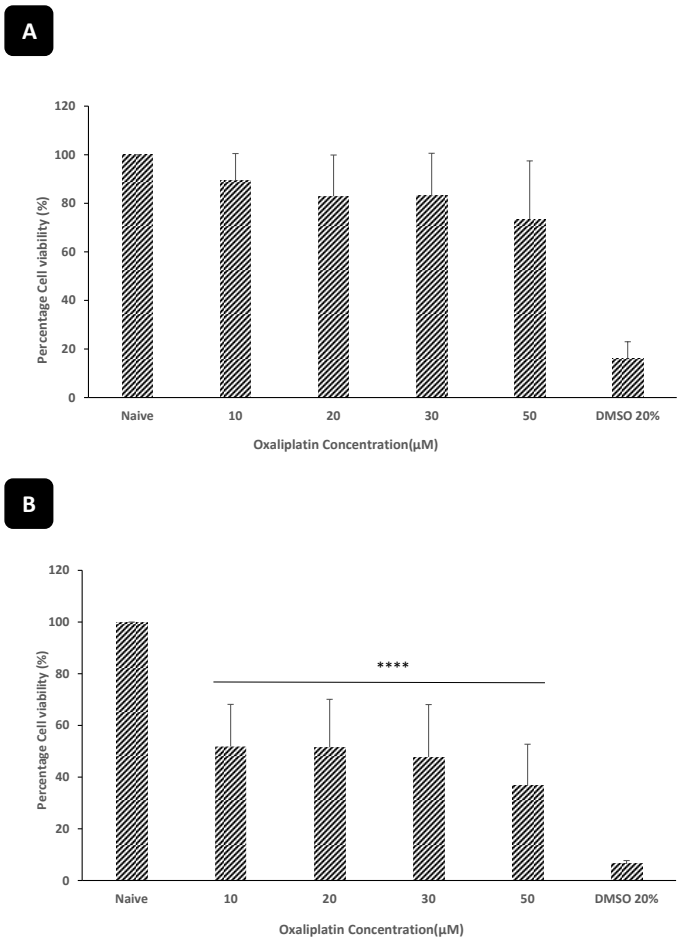

Figure 2: *Cell Viability (MTT Assay) of Breast carcinoma cell line (MCF-7) following treatment with oxaliplatin after (A) 24 hours and (B) 48 hours. MCF-7 cells were seeded with 5K per well and treated with a range of oxaliplatin concentration (10-50 µM). DMSO 20% was used as a positive control. Four independent experiments each with 12 replicates per experiment. Statistical analysis shows that the difference is significant from 10µM to 50µM and P < 0.0001.*

As compared to 5000 cells per well shown in **Figure 2**, the effects of oxaliplatin on a different MCF-7 cell density is highlighted in **Figure 3**. The cell viability of MCF-7 monolayer reduces to 70% at the highest oxaliplatin concentration ranging between 10-50µM after 24hrs treatment (**Figure 3A**) and to 40% after 48hrs (**Figure 3B**).

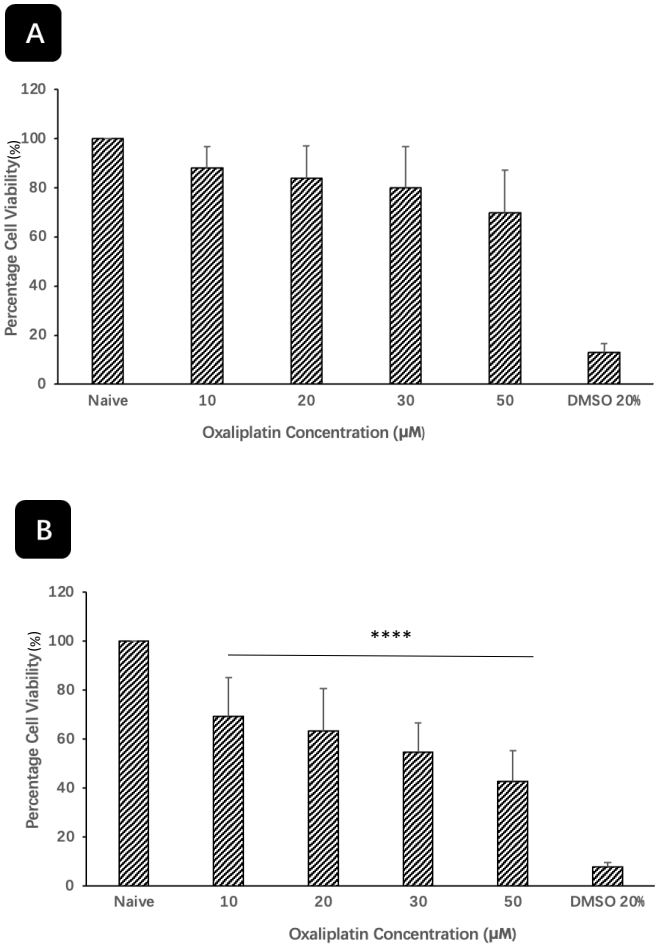

Figure 3: *Cell Viability (MTT Assay) of Breast carcinoma cell line (MCF-7) following treatment with oxaliplatin after (A) 24 hours and (B) 48 hours. MCF-7 cells were seeded with 7K per well and were treated with a range of oxaliplatin concentration (10-50 µM). DMSO 20% was used as a positive control. Four independent experiments each with 12 replicates per experiment. Significant difference from 10µM to 50µM, P<0.0001*

The cell viability of oxaliplatin was also studied in colorectal cell line, known as HCT116, seeding 5,000 and 7,000 cells per well. As shown in **Figure 4A**, it shows around 70% cell viability in 5,000 cell per well HCT-116 monolayers at the concentration range between 10-50µM oxaliplatin after 24hrs treatment. After 48hours, around 50% cell viability is shown with the most concentration of oxaliplatin as highlighted in **Figure 4B**.

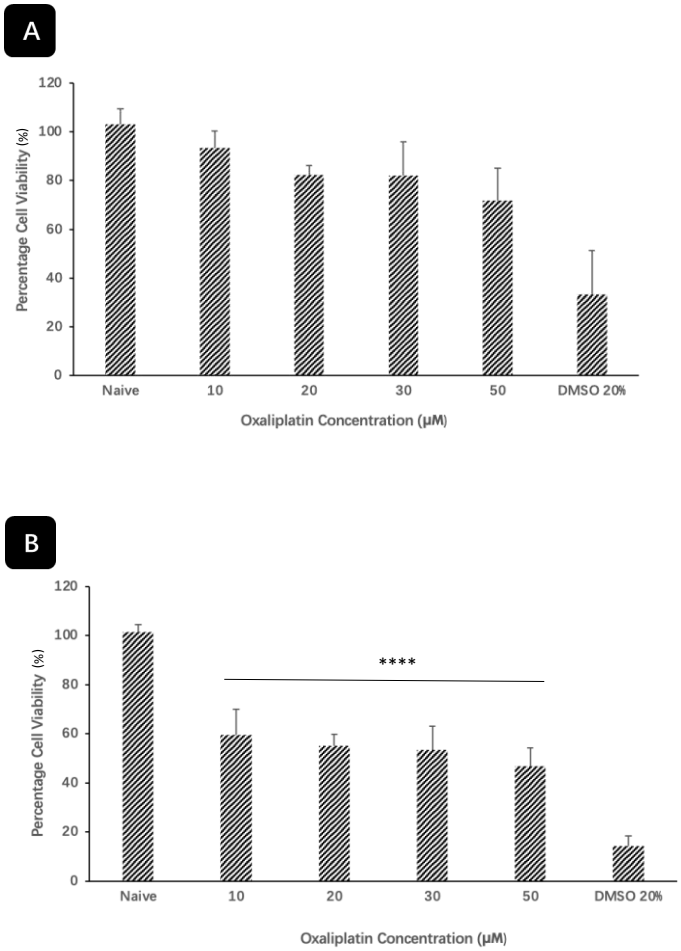

Figure 4: *Cell Viability (MTT Assay) of Human Colon cancer cell line (HCT-116) following treatment with oxaliplatin after (A) 24 hours and (B) 48 hours. HCT-116 cells were seeded at 5000 cells per well and treated with a range of oxaliplatin concentration (10-50 µM). DMSO 20% was used as a positive control. Four independent experiments each with 12 replicates per experiment were used. Significant difference from 10µM to 50µM, P<0.0001*

In term of 7000 cells per well HCT-116 cell viability decreases to 80% after 24hrs with oxaliplatin at 50µM concentration and to around to 50% after 48 hrs with most concentrations.

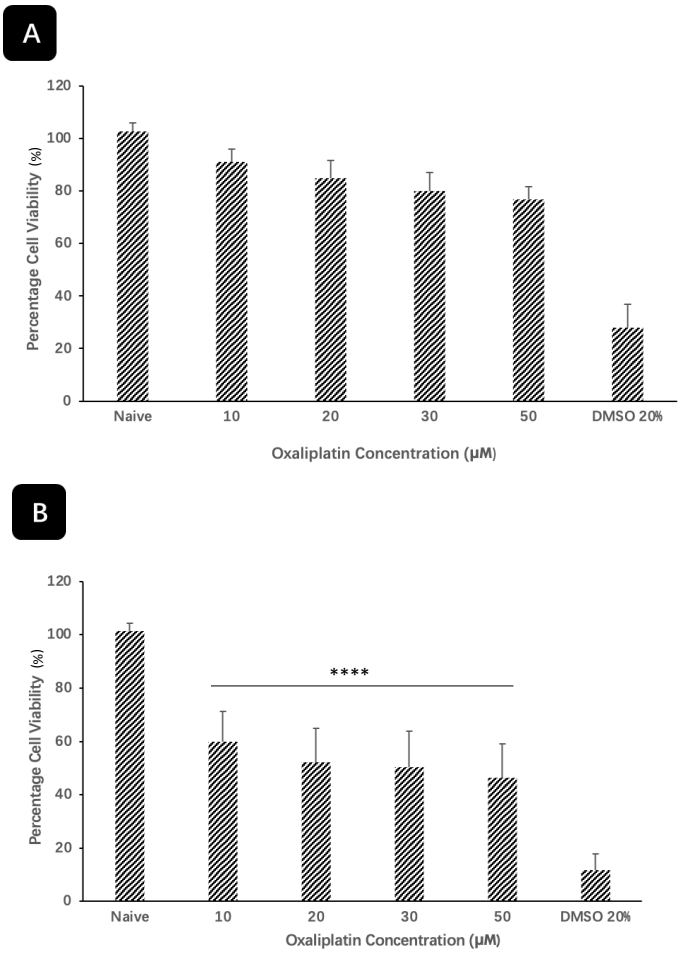

Figure 5: *Cell Viability (MTT Assay) of Human Colon cancer cell line (HCT-116) following treatment with oxaliplatin after (A) 24 hours and (B) 48 hours. HCT-116 cells were seeded with 7K per well and were treated with a range of oxaliplatin concentration (10-50 µM). DMSO 20% was used as a positive control. Four independent experiments each with 12 replicates per experiment. Statistics significant difference from 10µM to 50µM, P<0.0001*

4.1.2 Cell Viablity of Oxaliplatin and GO in 2D monolayer cells

Next, we looked at the ability of graphene oxide (GO) to deliver the anticancer drug oxaliplatin. GO was prepared using the modified Hummer's Methods *(Ali-Boucetta et al.,* 2013) and characterisation suggested the preparation of stable GO as shown in **Appendix 1**.We

have therefore, assessed the cell viability of different concentrations of GO and oxaliplatin on HCT116 cells after 24 and 48hr treatment. As shown in **Figure 6A** GO alone at the different concentration (5-50µg/mL) didn't show any reduction of cell viability to HCT116 cell lines after 24hrs of treatment. As expected oxaliplatin showed around 20% reduction in cell viability at different concentration (5-30 µM) of oxaliplatin. Interestingly, the combination of GO and oxaliplatin showed the same reduction of viability as oxaliplatin after 24hrs treatment as shown in **Figure 6A**. However, after 48hrs, it was clear that the combination of GO: oxaliplatin caused a dose-dependent tendency but the cell viability was no less than the group exposing oxaliplatin alone (**Figure 6B**). In addition, GO alone started showing a minimal cell viability (~10%) especially at the highest concentration of 50µg/ml. DMSO 20% is used as a positive control of toxicity and showed around 20% cell viability at 24 and 48hrs. Statistical difference was significant from 5µM to 30µM oxaliplatin, and in concentration of 5µM oxaliplatin : 50µg/ml GO, 10µM oxaliplatin : 50µg/ml GO, 15µM oxaliplatin : 50µg/ml GO, 20µM oxaliplatin : 50µg/ml GO and 30µM oxaliplatin : 50µg/ml GO, $p < 0.0001$.

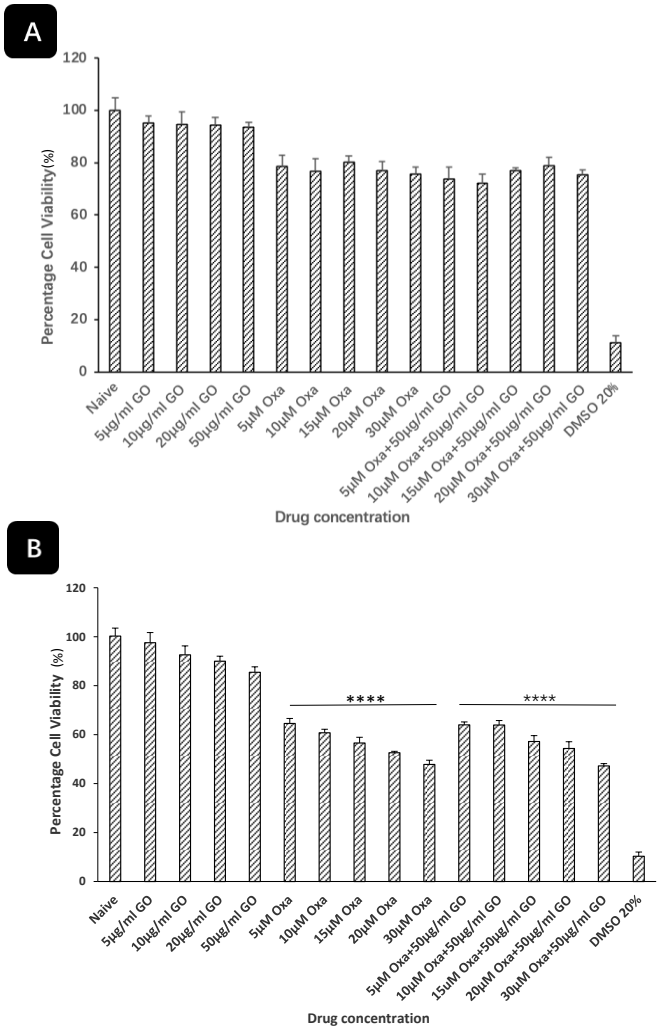

Figure 6: *Cell Viability (mLDH Assay) of Human Colon cancer cell line (HCT-116) following treatment with oxaliplatin and GO for (A) 24 hours and (B) 48 hours. HCT-116 cells were seeded at 7000 cells per well and treated with a range of concentration of oxaliplatin (5-30 µM), GO (5-50 µ m/ml) and the combination GO: Oxaliplatin. DMSO 20% was used as a positive control. Three independent experiments were performed each with 6 replicates per experiment. Statistics significant difference from 5µM to 30µM oxaliplatin, and in concentration of 5µM oxaliplatin : 50µg/ml GO, 10µM oxaliplatin : 50µg/ml GO, 15µM oxaliplatin : 50µg/ml GO, 20µM oxaliplatin : 50µg/ml GO and 30µM oxaliplatin : 50µg/ml GO , P<0.0001*

Figure 7A highlighted that exposing oxaliplatin alone was causing a slight dose- dependent tendency after 24hrs treatment. In addition, GO alone didn't cause any effects on MCF7 cell viability at the same time point. Interestingly, the combination of GO: oxaliplatin showed a significant cell viability decrease at the equivalent oxaliplatin alone

concentration. For instance, at 30µM of oxaliplatin alone is showing only 90% cell viability while the combination therapy is showing 70 %. These effects were further enhanced at the 48hrs time point with oxaliplatin alone at the highest concentration of 30µM showing 50% reduction in cell viability and the combination showing around 60% reduction in cell viability. This was also statistically significant from 5µM to 30µM oxaliplatin, and in concentration of 5µM oxaliplatin : 50µg/ml GO, 10µM oxaliplatin : 50µg/ml GO, 15µM oxaliplatin : 50µg/ml GO, 20µM oxaliplatin : 50µg/ml GO and 30µM oxaliplatin : 50µg/ml GO ($p < 0.0001$).

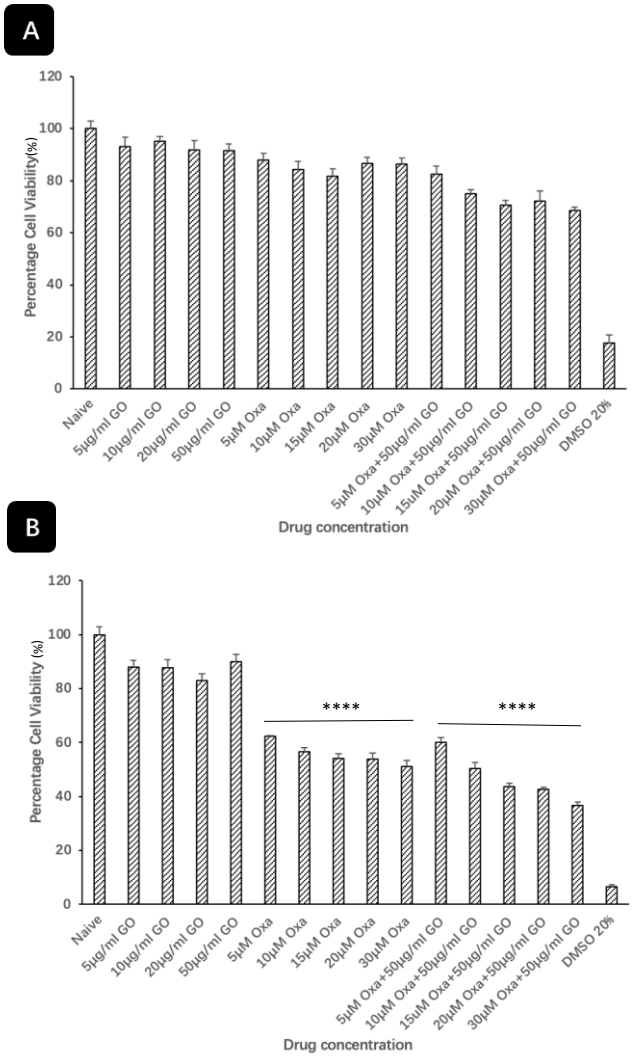

Figure 7: *Cell Viability (mLDH Assay) of Breast carcinoma cell line (MCF-7) following treatment with oxaliplatin and GO after (A) 24 hours and (B) 48 hours. MCF-7 cells were seeded with 7K per well and treated with a range of concentration 5-30 µM of oxaliplatin, 5-50 µ m/ml GO and combination. DMSO was used as a positive control. Four independent experiments each with 6 replicates per experiment. Statistics significant difference from 5µM to 30µM oxaliplatin, and in concentration of 5µM oxaliplatin : 50µg/ml GO, 10µM oxaliplatin : 50µg/ml GO, 15µM oxaliplatin : 50µg/ml GO, 20µM oxaliplatin : 50µg/ml GO and 30µM oxaliplatin : 50µg/ml GO , P<0.0001*

4.1.3 Cytotoxicity of Oxaliplatin and GO in 3D Spheroid

MCF7 multicellular spheroids were prepared using the liquid overlay method (Costa *et al.*, 2018) and were formed after 2 days of plating. MCF7 spheroids were formed on agar-based plates with different

concentration of oxaliplatin (5-30μM) and GO (5-50μg/mL) and combination of GO and oxaliplatin. As mentioned in the previous literature review, the range of spheroid diameter prefers to be formed from 100 to 600 μm (Friedrich, Ebner and Kunz-Schughart, 2007). According to the data of forming spheroids in several cell density experiments, as shown in **Figure 8**, the most appropriate cell density is 8000 per well and the diameter of spheroid tends to keep around 530-580μm (The scale bar in **Figure 8** is 1000μm).

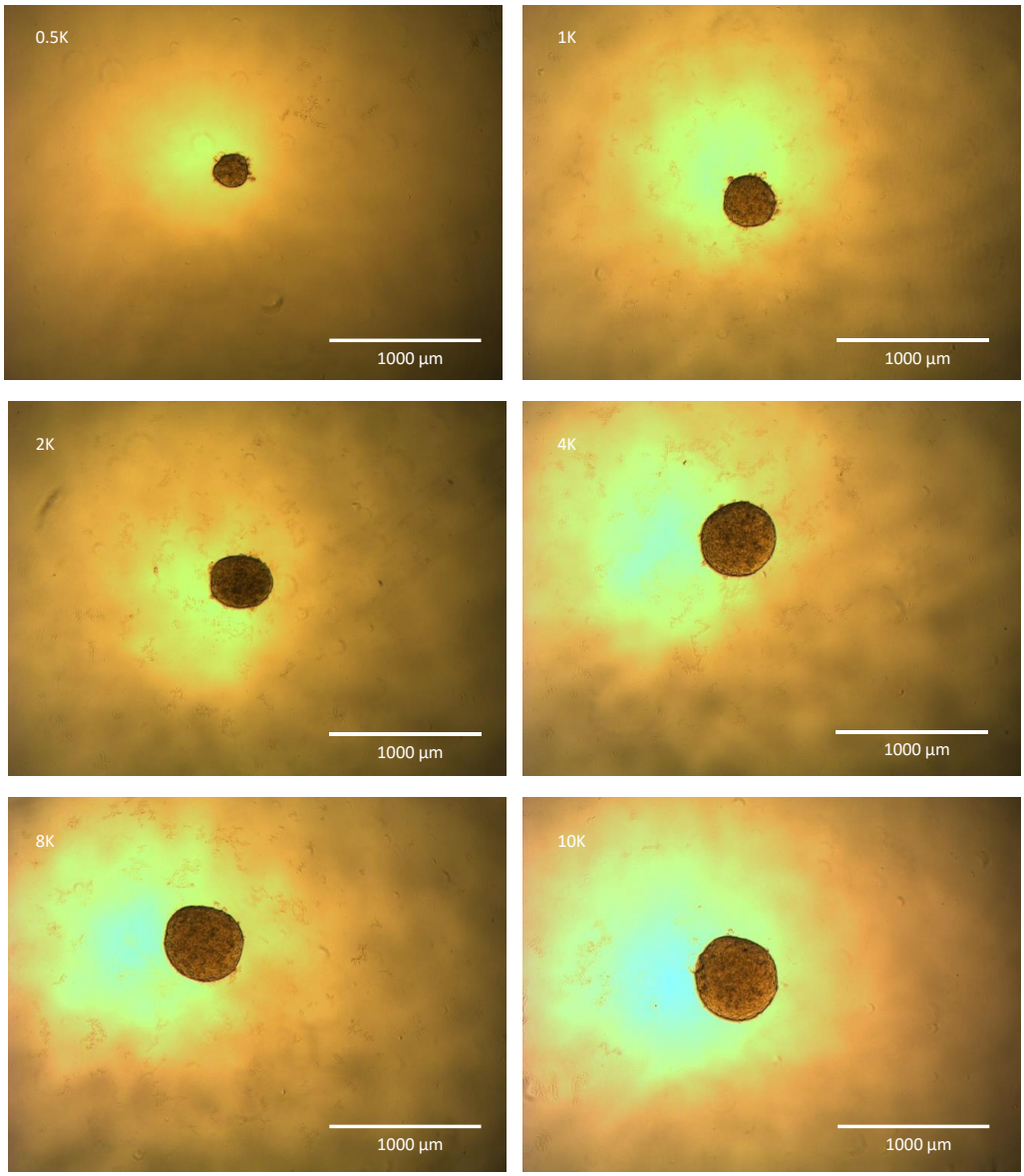

***Figure 8**: The images of spheroid morphology and size under microscope. MCF7 Cell density produced with 500, 1000, 2000, 4000, 8000 and 10000 per well after 72hrs by using 96-well plates.*

As shown in **Figure 9A**, there is not obvious change in the diameter of MCF-7 spheroids following their direct treatment on agar with a range of oxaliplatin concentration (5-30 µM), GO (5-50 µg/ml) and the combination GO: oxaliplatin after 24 hours. However, 48 hours

following treatment the MCF-7 spheroids are slightly inhibited with oxaliplatin and combination treatment as shown in **Figure 9B**. This was also statistically significant on 10µM oxaliplatin: 50µg/mL GO combination and 15µM oxaliplatin: 50µg/mL GO combination after 48hrs ($p<0.001$).

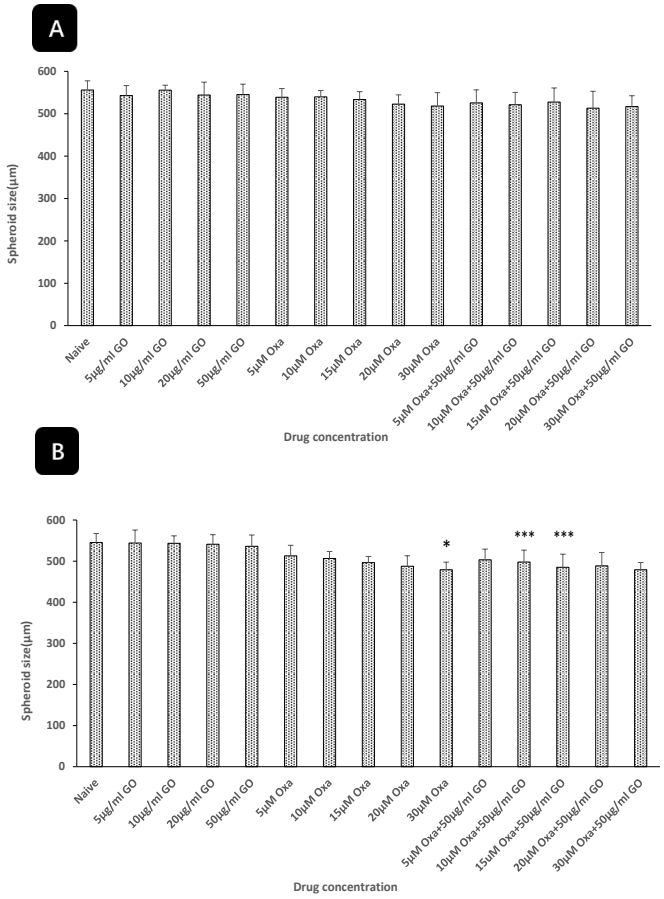

Figure 9: *3D Cell Diameter (Spheroid treatment) of Breast carcinoma cell line (MCF-7) following direct treatment on Agar with oxaliplatin and GO after (A) 24 hours and (B) 48 hours. MCF-7 cells were seeded on the agar at 8,000 per well and treated with a range of concentration 5-30 µM of oxaliplatin,5-50 µ m/ml GO and combination. Two independent experiments each with 3-6 replicates per experiment. Statistical analysis shows that the difference is significant on 10µM oxaliplatin: 50µg/mL GO combination and 15µM oxaliplatin: 50µg/mL GO combination, $P < 0.001$*

In consequence of the slight changes of 3D cell diameter (MCF-7

Spheroid treatment on agar), additional research was investigated and designed for further improved measurement and observation of inhibition.

Using the liquid overlay method, MCF7 spheroids were then treated on non-agar coated plates with different concentration of oxaliplatin (5-30μM) and GO (5-50μg/mL) and combination of GO and oxaliplatin. As seen in **Figure 10**, oxaliplatin and combination show inhibition of MCF-7 spheroids after treating 24 hours treatment (A), 48 hours (B) and 72 hours (C). However, spheroids treated with GO alone tend to be inhibited too. The impact of inhibition of spheroid growth by 20μg/mL and 50μg/mL GO is time dependent as shown in **Figure 10B** and **10C**. While inhibition is seen with oxaliplatin at 24hrs, this is further increased to 600μm and 800μm after 48hrs and 72hrs respectively. According to statistics analysis, the results of this study showed slight differences at 30μM oxaliplatin: 50μg/mL GO combination after 48hrs ($P<0.01$), showed significant differences among all the concentration of oxaliplatin: GO combination group after 72hrs ($P<0.0001$).

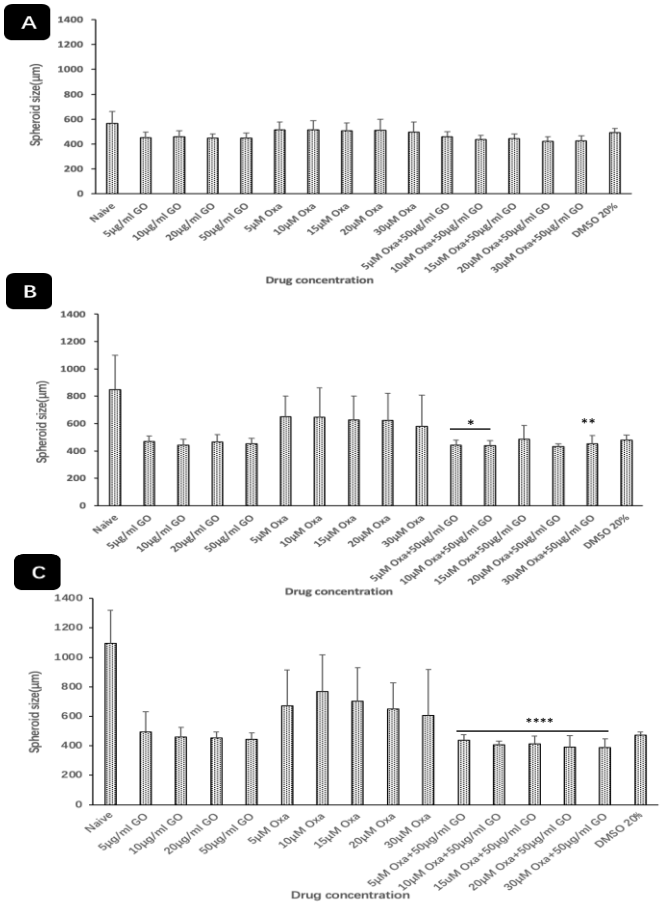

Figure 10: *Spheroids Diameter of Breast Carcinoma cell line (MCF-7) following treatment with oxaliplatin and GO for (A) 24 hours, (B) 48 hours and (C) 72 hours. MCF-7 spheroids (8,000 cells per well) were prepared using the liquid overlay method then treated in non-Agar coated plates with a range of concentration of oxaliplatin (5-30 µM), GO (5-50 µg/ml) and combination of GO: Oxaliplatin. Six independent experiments each with 3-6 replicates per experiment were performed. Slight differences at 5µM oxaliplatin: 50µg/mL GO combination,10µM oxaliplatin: 50µg/mL GO combination and 30µM oxaliplatin: 50µg/mL GO combination after 48hrs, and significant differences among all the concentration of oxaliplatin: GO combination group after 72hrs ($p<0.0001$).*

As seen in **Figure 10**, the most striking result to emerge from the data is that the form and diameter of spheroids changed significantly, and these variations were more beneficial in showing the cancer spheroids being inhibited by treatment.

5 Discussion

Current cell culture research has suggested that 3D spheroid is an ideal model to investigate the response and cell behaviour of tumours microenvironment. The establishment of an *in vitro* 3D cell culture model will help to fill up the gap between two-dimensional cell culture and animal experiments. Spheroids prefer to reveal accurate prediction of the response of genotype in tissue development and morphogenesis, cell differentiation, pathophysiological, drug and toxicity screening tests, and will help accelerate the research of drug delivery in the fields of cancer biology and tissue engineering (Kapałczyńska *et al.*, 2018). Much work is proposing the use of graphene oxide as a novel drug delivery system (Campbell *et al.*, 2019),(Liu, Cui and Losic, 2013), (Pan *et al.*, 2021), however it is unclear what GO is offering compared to other currently used drug delivery systems. To this end, it was thought to systematically study the delivery of an anticancer drug using GO as a delivery carrier in 2D and 3D cell culture. In view of this, different concentrations of the anticancer drug oxaliplatin was non-covalently complexed with GO and the cell viability exposing oxaliplatin was initially explored in breast (MCF7) and colorectal (HCT116) 2D cancer cell cultures.

First, the cell viability of treating oxaliplatin alone was assessed in MCF7 (breast) and HCT116 (colorectal) 2D cells using the MTT assay. This was done to determine the optimum cell density as well as the ideal concentration of oxaliplatin to be then complexed with graphene oxide. While both cell lines were affected by the different concentration of oxaliplatin, MCF7 was more sensitive to oxaliplatin especially after 48hrs treatment and in both cell densities (5000 & 7000 cells). It is important to highlight that oxaliplatin is platinum-based drug which exhibit its toxicity on cancer cells through DNA damage (Alcindor and Beauger, 2011). This was similar to what was found by Vivek *et al* in which nearly 50% cell viability was reported after MCF-7 cells (10000 cells per well) were exposed to 25 µM oxaliplatin after 48 hrs and the lowest of cell viability (34%) was exposed to 50 µM oxaliplatin after 48 hrs (Vivek *et al.*, 2014). Moreover, Alami *et al*., described that 50% cell viability of MCF7 was revealed in nearly 17 µM oxaliplatin after 48 hrs (Alami *et al.*, 2007). Compare our findings to that in literatures with studies that the cell viability of MCF7 monolayer reduces to 50% at the same concertation ranging between 17-25 µM. Similar results were also reported by

others for HCT116, which is shown that 25 µM oxaliplatin has 50% cell viability after exposing 48hrs (Tabasi *et al.*, 2021).

Then, graphene oxide was prepared using the modified Hummer's method as described by Ali-Boucetta *et al* (Ali-Boucetta *et al.*, 2013). As expected, GO showed to be of stable dispersion at 1mg/mL (Appendix 1, **Figure S1**) and as expected exhibited a negative charge (Appendix 1, **Figure S2**) due to hydroxyl and carboxyl groups as well as a sharp absorption peak around 230nm (Appendix 1, **Figure S3**) as suggested by others (Mei *et al.*, 2010). GO was then complexed with oxaliplatin at room temperature and the cytotoxicity of the complexes was indirectly assessed using the modified LDH assay to avoid any interference of GO with the assay as reported by Ali-Boucetta *et al* (Ali-Boucetta *et al.*, 2011) for carbon-based nanomaterials. GO: oxaliplatin complexes exhibited some cytotoxicity in HCT116 after 48hrs but this was not as strong as that observed with the drug alone. As expected GO alone exhibited no toxicity on both HCT116 cells. This is similar to what previously reported by others on different cells (Ali-Boucetta *et al*., 2013),(Jasim, Lozano and Kostarelos, 2016),(Bengtson *et al.*, 2016). Interestingly, treatment of MCF7 with GO: oxaliplatin complexes exhibited a reduction of cell viability

(30%) as compared to oxaliplatin alone (10%) after 24hrs (**Figure 7**). This was further enhanced to 50% reduction in cell survival with the complexes after 48hrs. It is believed that GO could have tethered oxaliplatin inside the cells leading to an enhanced cytotoxicity of oxaliplatin inside the cells and hence acted as an efficient drug delivery system. While we believe this is the first study that looked at the effect of GO: oxaliplatin non-covalent complexes, others have used functionalised graphene oxide nanosheets by human serum albumin (HSA) nanoparticles (Farnaz *et al.*, 2018) and platinum anticancer drugs based functionalized graphene oxide nanoparticles (Wei *et al*., 2021) and described similar results. For instance, Farnaz *et al* found that, due to the specific properties of GO-NSs, FGO-NSs has lower cytotoxicity and better performance on loading drugs and entrapping than GO-NSs, which could extend the release time as an ideal nanoparticle for deliver anticancer drugs. GO has been previously suggested to deliver different anticancer drugs such as doxorubicin (Yaghoubi *et al.*, 2022), (Yang *et al.*, 2020), (Zhou, Zhou and Xing, 2014), methotrexate (Abdelhamid and Hussein, 2021), gemcitabine (X. Wei *et al.*, 2021). In addition, Rosili *et al.* described that GO potentiate the anticancer effects of cisplatin, another platinum-based drug, in lung (A549) carcinoma cells (Rosli *et al.*,

2019). Others have also described the benefits of using PEGylated GO for the co-delivery of cisplatin and doxorubicin (Pei *et al.*, 2020). pH- and thermo-sensitive GO-PNVCL-PGA could also release the oxaliplatin in targeted site efficiently (Kazempour *et al*., 2019). Hyaluronyl-modified rGO would enhance the doxorubicin uptake and has stability and safety as drug delivery nanocarrier (Miao *et al*., 2013).

Since the effects of cell viability in 2D monolayer were more pronounced in MCF-7, the rest of the study focused on the effect of the complexes on MCF-7 spheroids. These were prepared using the liquid overlay method (Metzger *et al.*, 2011). 3D spheroids are an ideal model to replicate the *in vivo* tumour conditions due to the similarities between spheroids and solid tumour. These include the spatial structure, physiological activity and the sensitivity or resistance mechanism for anticancer drugs (Mehta *et al.*, 2012), (Costa *et al.*, 2016). The cell-cell connections in spheroid could change the mode of responding, metabolism and even gene expression, compared with monolayer cancer cells, which shows different response to drugs. For example, V79 spheroid would reduce the efficiency of etoposide and ionizing radiation (Oloumi *et al.*, 2002). The spheroid could generate

the matrix which might mimic the drugs or other substances transferred in cell-matrix microenvironment (Dingle *et al.*, 2015). Therefore, it was important to investigate the ability of GO to diffuse inside the MCF-7 spheroids in an attempt to assess their effectiveness as a drug delivery system. While the GO: oxaliplatin complexes caused a reduction in the diameter of MCF-7 spheroids after 48hrs treatment, it was unclear why the GO alone was also toxic to spheroids. This was however previously reported by Wang *et al*, who stated that GO inhibit cell proliferation and induces apoptotic cell death in glioblastoma stem cell-like spheroids (Wang *et al.*, 2020). Further work is therefore warranted to understand if the sharp edges of GO act as nanoswords and destroy the spheroid rim and hence why oxaliplatin showed a better effect in the complexes compared to alone. Moreover, others (de Lázaro *et al.*, 2021) found that GO alone translocated deep within glioblastoma U-87 MG spheroids which could also mean that GO could have acted here as an efficient drug delivery system and delivered oxaliplatin though further work is required to proof this hypothesis. Graphene oxide plus Doxorubicin could raise the efficacy of cell apoptosis and inhibit obviously the growth of BT474 and MCF7 breast cancer stem cells *in vitro* (Ebrahimi *et al.*,2021).It is however important to highlight that the

characteristics and morphology of spheroids could also affect how the drug delivery system interacts with the spheroid for example their compactness which would be determined by the cell type (Han, Kwon and Kim, 2021). Therefore, it is important to study the translocation of the delivery system in different type of spheroids. In addition, the concentration of oxaliplatin should be revisited as the concentration could be effective in 2D monolayers but needs to be increased for 3D cultures. In a similar way, the incubation time should also be optimised. Meanwhile, further direct cytotoxicity assays should be designed and assessed on 2D monolayer cells and 3D spheroid to provide more observations regarding the effects of GO complexed with oxaliplatin.

6 Conclusion

The present study was designed to determine the effect of GO complexed with oxaliplatin, on preventing the growth of HCT-116 and MCF-7 cancer cells as 2D and 3D culture models. While GO showed to be non-toxic at the concentration used, the cytotoxicity on 2D monolayer cancer cells, oxaliplatin complexed with GO inhibited the growth of MCF-7 and HCT-116 cells. The findings of this research also

provide insights for the delivery of a model anticancer drug in 3D spheroid model. The cytotoxic effects of GO complexed with oxaliplatin on spheroid were similar to those on 2D monolayer, however GO alone also effected spheroid size. This work has highlighted that GO could support the increased penetration and deliver of oxaliplatin deeper in the 3D tumour models. The insights gained from this study may assist design of an excellent delivery system based on GO.

7 Future work

- Increasing the concentration of oxaliplatin in 3D spheroid work
- Increasing the time point of assessment in 3D spheroid work
- Analysis of the spheroids using Annexin V PI to investigate the stages of apoptosis
- Imaging of GO inside the spheroids using transmission electron microscopy (TEM) sections
- Study the effect of GO: oxaliplatin on different spheroids in order to see if the morphology plays a role in the translocation process
- Assessing the cytotoxicity via direct cytotoxicity assays on monolayer cells and spheroid

List of References

Abdelhalim, A.O.E. *et al.* (2022) ‘Graphene oxide enriched with oxygen-containing groups: on the way to an increase of antioxidant activity and biocompatibility’, *Colloids and Surfaces B: Biointerfaces*, 210, p. 112232. doi:10.1016/j.colsurfb.2021.112232.

Abdelhamid, H.N. and Hussein, K.H. (2021) ‘Graphene Oxide as a Carrier for Drug Delivery of Methotrexate’, *Biointerface Research in Applied Chemistry*, 11(6), pp. 14726–14735. doi:10.33263/BRIAC116.1472614735.

Abdolahinia, E.D. *et al.* (2019) ‘Enhanced penetration and cytotoxicity of metformin and collagenase conjugated gold nanoparticles in breast cancer spheroids’, *Life Sciences*, 231, p. 116545. doi:10.1016/j.lfs.2019.116545.

Achilli, T. *et al.* (2012) ‘Advances in the formation, use and understanding of multi-cellular spheroids’, *Expert Opinion on Biological Therapy*, 12(10), p. 1347-1360. doi: 10.1517/14712598.2012.707181.

Alami, N. *et al.* (2007) ‘Comparative preclinical antiproliferative activity of lobaplatin vs cisplatin, carboplatin, oxaliplatin and satraplatin in breast and ovarian cancers’, *Cancer Research*, 67(9_Supplement), p. 4780.

Alcindor, T. and Beauger, N. (2011) ‘Oxaliplatin: a review in the era of molecularly targeted therapy’, *Current Oncology*, 18(1), pp. 18–25.

Ali-Boucetta, H. *et al.* (2011) ‘Cellular uptake and cytotoxic impact of chemically functionalized and polymer-coated carbon nanotubes’, *Small (Weinheim an Der Bergstrasse, Germany)*, 7(22), pp. 3230–3238. doi:10.1002/smll.201101004.

Ali-Boucetta, H. *et al.* (2013a) ‘Purified Graphene Oxide Dispersions Lack In Vitro Cytotoxicity and In Vivo Pathogenicity’, *Advanced Healthcare Materials*, 2(3), pp. 433–441. doi:10.1002/adhm.201200248.

Ali-Boucetta, H. *et al.* (2013b) ‘Purified Graphene Oxide Dispersions Lack In Vitro Cytotoxicity and In Vivo Pathogenicity’, *Advanced Healthcare Materials*, 2(3), pp. 433–441. doi:10.1002/adhm.201200248.

Antoni, D *et al.* (2015) ‘Three-Dimensional Cell Culture: A Breakthrough in Vivo’, *Int. J. Mol. Sci. 2015, 16, 5517-5527; doi:10.3390/ijms16035517*

Asthana, A. and Kisaalita, W.S. (2012) ‘Microtissue size and hypoxia in HTS with 3D cultures’, *Drug Discovery Today*, 17(15), pp. 810–817. doi:10.1016/j.drudis.2012.03.004.

Barahuie, F. *et al.* (2017) ‘Graphene oxide as a nanocarrier for controlled release and targeted delivery of an anticancer active agent, chlorogenic acid’, *Materials Science and Engineering: C*, 74, pp. 177–185. doi:10.1016/j.msec.2016.11.114.

Baek,N . *et al.* (2016) ‘Monitoring the effects of doxorubicin on 3D-spheroid tumor cells in real-time’, *OncoTargets and Therapy*,9, 7207-7218, doi: 10.2147/OTT.S112566.

Bengtson, S. *et al.* (2016) ‘No cytotoxicity or genotoxicity of graphene and graphene oxide in murine lung epithelial FE1 cells in vitro’, *Environmental and Molecular Mutagenesis*, 57(6), pp. 469–482. doi:10.1002/em.22017.

Bierwolf, J. *et al.* (2011) ‘Primary rat hepatocyte culture on 3D nanofibrous polymer scaffolds for toxicology and pharmaceutical research’, *Biotechnology and Bioengineering*, 108(1), pp. 141-150. doi: 10.1002/bit.22924.

Borandeh, S. *et al.* (2021) ‘Graphene Family Nanomaterials in Ocular Applications: Physicochemical Properties and Toxicity’, *Chemical Research in Toxicology*, 34(6), pp. 1386–1402. doi:10.1021/acs.chemrestox.0c00340.

Breslin, S. and O’Driscoll, L. (2013) ‘Three-dimensional cell culture: the missing link in drug discovery’, *Drug Discovery Today*, 18(5), pp. 240–249. doi:10.1016/j.drudis.2012.10.003.

Campbell, E. *et al.* (2019) ‘Graphene Oxide as a Multifunctional Platform for Intracellular Delivery, Imaging, and Cancer Sensing’, *Scientific Reports*, 9(1), p. 416. doi:10.1038/s41598-018-36617-4.

Carlsson, J. and Yuhas, J.M. (1984) ‘Liquid-Overlay Culture of Cellular Spheroids’, in Acker, H. et al. (eds) *Spheroids in Cancer Research: Methods and Perspectives*. Berlin, Heidelberg: Springer, pp. 1–23. doi:10.1007/978-3-642-82340-4_1.

Cassidy, J. and Misset, J.-L. (2002) ‘Oxaliplatin-related side effects: characteristics and management’, *Seminars in oncology*, 29(5 Suppl 15), pp. 11–20. doi:10.1053/sonc.2002.35524.

Chang, Y. *et al.* (2011) ‘In vitro toxicity evaluation of graphene oxide on A549 cells’, *Toxicology Letters*, 200(3), pp. 201–210. doi:10.1016/j.toxlet.2010.11.016.

Costa, E.C. *et al.* (2016) '3D tumor spheroids: an overview on the tools and techniques used for their analysis', *Biotechnology Advances*, 34(8), pp. 1427–1441. doi:10.1016/j.biotechadv.2016.11.002.

Costa, E.C. *et al.* (2018) 'Spheroids Formation on Non-Adhesive Surfaces by Liquid Overlay Technique: Considerations and Practical Approaches', *Biotechnology Journal*, 13(1), p. 1700417. doi:10.1002/biot.201700417.

Couvreur, P. (2013) 'Nanoparticles in drug delivery: Past, present and future', *Advanced Drug Delivery Reviews*, 65(1), pp. 21–23. doi:10.1016/j.addr.2012.04.010.

Dadgar, N. (2020) 'A microfluidic platform for cultivating ovarian cancer spheroids and testing their responses to chemotherapies', *Microsystems & Nanoengineering*, 6 (1), pp. 1-12. doi: 10.1038/s41378-020-00201-6.

De Jong, W.H. and Borm, P.J. (2008) 'Drug delivery and nanoparticles: Applications and hazards', *International Journal of Nanomedicine*, 3(2), pp. 133–149.

Del Duca, D., Werbowetski, T. and Del Maestro, R.F. (2004) 'Spheroid Preparation from Hanging Drops: Characterization of a Model of Brain Tumor Invasion', *Journal of Neuro-Oncology*, 67(3), pp. 295–303. doi:10.1023/B:NEON.0000024220.07063.70.

Dingle, Y.-T.L. *et al.* (2015) 'Three-Dimensional Neural Spheroid Culture: An In Vitro Model for Cortical Studies', *Tissue Engineering. Part C, Methods*, 21(12), pp. 1274–1283. doi:10.1089/ten.TEC.2015.0135.

Ebrahimi, M. (no date) 'The synergistic anticancer traits of graphene oxide plus doxorubicin against BT474 and MCF7 breast cancer stem cells in vitro', p. 23.

Eckel, F. *et al.* (2002) '[Prevention of oxaliplatin-induced neuropathy by carbamazepine. A pilot study]', *Deutsche medizinische Wochenschrift (1946)*, 127(3), pp. 78–82. doi:10.1055/s-2002-19594.

Extra, J.M. *et al.* (1998) 'Pharmacokinetics and safety profile of oxaliplatin', *Seminars in oncology*, 25(2 Suppl 5), pp. 13–22.

Farnaz, R. *et al.* (2018) 'Colloidal HSA – Graphene oxide nanosheets for sustained release of oxaliplatin: Preparation, release mechanism, cytotoxicity and electrochemical approaches', *Colloids and Surfaces B: Biointerfaces*, 171, pp. 10–16. doi:10.1016/j.colsurfb.2018.07.010.

Friedrich, J., Ebner, R. and Kunz-Schughart, L.A. (2007) ‘Experimental anti-tumor therapy in 3-D: Spheroids – old hat or new challenge?’, *International Journal of Radiation Biology*, 83(11–12), pp. 849–871. doi:10.1080/09553000701727531.

Froehlich, K. *et al.* (2016) ‘Generation of Multicellular Breast Cancer Tumor Spheroids: Comparison of Different Protocols’, *Journal of Mammary Gland Biology and Neoplasia*, 21(3), pp. 89–98. doi:10.1007/s10911-016-9359-2.

Ganesan, K. *et al.* (2020) ‘Green synthesis of Copper oxide nanoparticles decorated with graphene oxide for anticancer activity and catalytic applications’, *Arabian Journal of Chemistry*, 13(8), pp. 6802–6814. doi:10.1016/j.arabjc.2020.06.033.

Grothey, A. (2003) ‘Oxaliplatin-safety profile: neurotoxicity’, *Seminars in Oncology*, 30, pp. 5–13. doi:10.1016/S0093-7754(03)00399-3.

Gu, Z. *et al.* (2019) ‘Graphene-Based Smart Platforms for Combined Cancer Therapy’, *Advanced Materials*, 31(9), p. 1800662. doi:10.1002/adma.201800662.

Han, S.J., Kwon, S. and Kim, K.S. (2021) ‘Challenges of applying multicellular tumor spheroids in preclinical phase’, *Cancer Cell International*, 21(1), p. 152. doi:10.1186/s12935-021-01853-8.

Handschel, J.G. *et al.* (2007) ‘Prospects of micromass culture technology in tissue engineering’, *Head & Face Medicine*, 3(1), p. 4. doi:10.1186/1746-160X-3-4.

Hu, Z. *et al.* (2012) ‘Visible light driven photodynamic anticancer activity of graphene oxide/TiO2 hybrid’, *Carbon*, 50(3), pp. 994–1004. doi:10.1016/j.carbon.2011.10.002.

Jasim, D.A., Lozano, N. and Kostarelos, K. (2016) ‘Synthesis of few-layered, high-purity graphene oxide sheets from different graphite sources for biology’, *2D Materials*, 3(1), p. 014006. doi:10.1088/2053-1583/3/1/014006.

Kapałczyńska, M. *et al.* (2018) ‘2D and 3D cell cultures – a comparison of different types of cancer cell cultures’, *Archives of Medical Science : AMS*, 14(4), pp. 910–919. doi:10.5114/aoms.2016.63743.

Karlsson, H. *et al.* (2012) ‘Loss of cancer drug activity in colon cancer HCT-116 cells during spheroid formation in a new 3-D spheroid cell culture system’, *Experimental Cell Research*, 318(13), pp. 1577–1585. doi:10.1016/j.yexcr.2012.03.026.

Kausar, A. (2021) ‘Conjugated Polymer/Graphene Oxide Nanocomposites—State-of-the-Art’, *Journal of Composites Science*, 5(11), p. 292. doi:10.3390/jcs5110292.

Kavitha, T., Abdi, S.I.H. and Park, S.-Y. (2013) ‘pH-Sensitive nanocargo based on smart polymer functionalized graphene oxide for site-specific drug delivery’, *Physical Chemistry Chemical Physics*, 15(14), pp. 5176–5185. doi:10.1039/C3CP00008G.

Kazempour, M. *et al.* (2019) ‘Synthesis and characterization of dual pH-and thermo-responsive graphene-based nanocarrier for effective anticancer drug delivery’, *Journal of Drug Delivery Science and Technology*, 54, p. 101158. doi:10.1016/j.jddst.2019.101158.

de Lázaro, I. *et al.* (2021) ‘Deep Tissue Translocation of Graphene Oxide Sheets in Human Glioblastoma 3D Spheroids and an Orthotopic Xenograft Model’, *Advanced Therapeutics*, 4(1), p. 2000109. doi:10.1002/adtp.202000109.

Liu, J. *et al.* (2017) ‘Comparison of nanomedicine-based chemotherapy, photodynamic therapy and photothermal therapy using reduced graphene oxide for the model system’, *Biomaterials Science*, 5(2), pp. 331–340. doi:10.1039/C6BM00526H.

Liu, J., Cui, L. and Losic, D. (2013) ‘Graphene and graphene oxide as new nanocarriers for drug delivery applications’, *Acta Biomaterialia*, 9(12), pp. 9243–9257. doi:10.1016/j.actbio.2013.08.016.

Mahmood, T. *et al.* (2014) ‘Adhesion-mediated signal transduction in human articular chondrocytes: the influence of biomaterial chemistry and tenascin-C’, *Experimental Cell Research*, 301 (2), pp. 179-188. doi: 10.1016/j.yexcr.2004.07.027.

Mathé, G. *et al.* (1989) ‘Oxalato-platinum or 1-OHP, a third-generation platinum complex: an experimental and clinical appraisal and preliminary comparison with cis-platinum and carboplatinum’, *Biomedicine & Pharmacotherapy*, 43(4), pp. 237–250. doi:10.1016/0753-3322(89)90003-6.

Mehta, G. *et al.* (2012) ‘Opportunities and challenges for use of tumor spheroids as models to test drug delivery and efficacy’, *Journal of Controlled Release*, 164(2), pp. 192–204. doi:10.1016/j.jconrel.2012.04.045.

Mei, Q. *et al.* (2010) ‘Highly efficient photoluminescent graphene oxide with tunable surface properties’, *Chemical Communications*, 46(39), pp. 7319–7321. doi:10.1039/C0CC02374D.

Metzger, W. *et al.* (2011) ‘The liquid overlay technique is the key to formation of co-culture spheroids consisting of primary osteoblasts, fibroblasts and endothelial cells’, *Cytotherapy*, 13(8), pp. 1000–1012. doi:10.3109/14653249.2011.583233.

Miao, W. *et al.* (2013) ‘Cholesteryl hyaluronic acid-coated, reduced graphene oxide nanosheets for anti-cancer drug delivery’, *Biomaterials*, 34(37), pp. 9638–9647. doi:10.1016/j.biomaterials.2013.08.058.

Mittler, F . *et al.* (2017) ‘High-Content Monitoring of Drug Effects in a 3D Spheroid Model’, *Frontiers in Oncology*, 7, pp. doi:10.3389/fonc.2017.00293.

Mo, R. and Gu, Z. (2016) ‘Tumor microenvironment and intracellular signal-activated nanomaterials for anticancer drug delivery’, *Materials Today*, 19(5), pp. 274–283. doi:10.1016/j.mattod.2015.11.025.

Oloumi, A. *et al.* (2002) ‘Identification of genes differentially expressed in V79 cells grown as multicell spheroids’, *International Journal of Radiation Biology*, 78(6), pp. 483–492. doi:10.1080/09553000210122299.

Pan, H. *et al.* (2016) ‘Fabrication and Characterization of Taurine Functionalized Graphene Oxide with 5-Fluorouracil as Anticancer Drug Delivery Systems’, *Nanoscale Research Letters*, 16(1), p. 84. doi:10.1186/s11671-021-03541-y.

Patra, B. *et al.* (2021) ‘Drug testing and flow cytometry analysis on a large number of uniform sized tumor spheroids using a microfluidic device’, *Scientific Reports* .6:21061. DOI: 10.1038/srep21061.

Pei, X. *et al.* (2020) ‘PEGylated nano-graphene oxide as a nanocarrier for delivering mixed anticancer drugs to improve anticancer activity’, *Scientific Reports*, 10(1), p. 2717. doi:10.1038/s41598-020-59624-w.

Rosli, N.F. *et al.* (2019) ‘Graphene Oxide Nanoplatelets Potentiate Anticancer Effect of Cisplatin in Human Lung Cancer Cells’, *Langmuir*, 35(8), pp. 3176–3182. doi:10.1021/acs.langmuir.8b03086.

Sambale, F. *et al.* (2015) ‘Three dimensional spheroid cell culture for nanoparticle safety testing’, *Journal of Biotechnology*, 205, pp. 120–129. doi:10.1016/j.jbiotec.2015.01.001.

Sengupta, R. *et al.* (2011) ‘A review on the mechanical and electrical properties of graphite and modified graphite reinforced polymer composites’, *Progress in Polymer Science*, 36(5), pp. 638–670. doi:10.1016/j.progpolymsci.2010.11.003.

Shao, L. *et al.* (2017) ‘Mesoporous Silica Coated Polydopamine Functionalized Reduced Graphene Oxide for Synergistic Targeted Chemo-Photothermal Therapy’, *ACS Applied Materials & Interfaces*, 9(2), pp. 1226–1236. doi:10.1021/acsami.6b11209.

Sturala, J. *et al.* (2018) ‘Chemistry of Graphene Derivatives: Synthesis, Applications, and Perspectives’, *Chemistry – A European Journal*, 24(23), pp. 5992–6006. doi:10.1002/chem.201704192.

Sun, X. *et al.* (2008) ‘Nano-graphene oxide for cellular imaging and drug delivery’, *Nano Research*, 1(3), pp. 203–212. doi:10.1007/s12274-008-8021-8.

Tabasi, H. *et al.* (2021) ‘pH-responsive and CD44-targeting by Fe3O4/MSNs-NH2 nanocarriers for Oxaliplatin loading and colon cancer treatment’, *Inorganic Chemistry Communications*, 125, p. 108430. doi:10.1016/j.inoche.2020.108430.

Tewari, K. and Manetta, A. (1999) ‘In vitro chemosensitivity testing and mechanisms of drug resistance’, *Current Oncology Reports*, 1(1), pp. 77–84. doi:10.1007/s11912-999-0014-6.

Vivek, R. *et al.* (2014) ‘Oxaliplatin-chitosan nanoparticles induced intrinsic apoptotic signaling pathway: A “smart” drug delivery system to breast cancer cell therapy’, *International Journal of Biological Macromolecules*, 65, pp. 289–297. doi:10.1016/j.ijbiomac.2014.01.054.

Wang, A. *et al.* (2013) ‘Role of surface charge and oxidative stress in cytotoxicity and genotoxicity of graphene oxide towards human lung fibroblast cells’, *Journal of applied toxicology: JAT*, 33(10), pp. 1156–1164. doi:10.1002/jat.2877.

Wang, X. *et al.* (2020) ‘Graphene oxide suppresses the growth and malignancy of glioblastoma stem cell-like spheroids via epigenetic mechanisms’, *Journal of Translational Medicine*, 18(1), p. 200. doi:10.1186/s12967-020-02359-z.

Wei, L. *et al.* (2021a) ‘Functionalized Graphene Oxide as Drug Delivery Systems for Platinum Anticancer Drugs’, *Journal of Pharmaceutical Sciences*, 110(11), pp. 3631–3638. doi:10.1016/j.xphs.2021.07.009.

Wei, L. *et al.* (2021b) ‘Functionalized Graphene Oxide as Drug Delivery Systems for Platinum Anticancer Drugs’, *Journal of Pharmaceutical Sciences*, 110(11), pp. 3631–3638. doi:10.1016/j.xphs.2021.07.009.

Wei, X. *et al.* (2021) ‘Engineering of gemcitabine coated nano-graphene oxide

sheets for efficient near-infrared radiation mediated in vivo lung cancer photothermal therapy', *Journal of Photochemistry and Photobiology B: Biology*, 216, p. 112125. doi:10.1016/j.jphotobiol.2021.112125.

Yaghoubi, F. *et al.* (2022) 'A functionalized graphene oxide with improved cytocompatibility for stimuli-responsive co-delivery of curcumin and doxorubicin in cancer treatment', *Scientific Reports*, 12(1), p. 1959. doi:10.1038/s41598-022-05793-9.

Yang, Z. *et al.* (2020) 'Simultaneous Delivery of antimiR-21 and Doxorubicin by Graphene Oxide for Reducing Toxicity in Cancer Therapy', *ACS Omega*, 5(24), pp. 14437–14443. doi:10.1021/acsomega.0c01010.

Yip, D. and Cho.C. (2013) 'A multicellular 3D heterospheroid model of liver tumor and stromal cells in collagen gel for anti-cancer drug testing', *Biochemical and Biophysical Research Communications*, 433(3), pp. 327-332. doi: 10.1016/j.bbrc.2013.03.008.

Zhang, X. *et al.* (2012) 'A comparative study of cellular uptake and cytotoxicity of multi-walled carbon nanotubes, graphene oxide, and nanodiamond', *Toxicology Research*, 1(1), pp. 62–68. doi:10.1039/c2tx20006f.

Zhou, T., Zhou, X. and Xing, D. (2014) 'Controlled release of doxorubicin from graphene oxide based charge-reversal nanocarrier', *Biomaterials*, 35(13), pp. 4185–4194. doi:10.1016/j.biomaterials.2014.01.044.

Zuchowska, A. *et al.* (2020) '3D and 2D cell models in a novel microfluidic tool for evaluation of highly chemically and microbiologically pure graphene oxide (GO) as an effective drug carrier', *Sensors and Actuators B: Chemical*, 302, p. 127064. doi:10.1016/j.snb.2019.127064.

Appendix 1

Figure S1: *Digital photograph of the dispersion condition of graphene oxide dispersion after 15 minutes of sonication in a water bath. The concentration of GO shown is 1mg/mL in water.*

According to the results, the Zeta potential of graphene oxide solution in **Figure S2** which is dispersed in sterile water at room temperature and pH was around 7 should be 40.7±6.8 mV and STD was 1.14. Interestingly, Zeta potential was investigated with no correlation to the solution concentration.

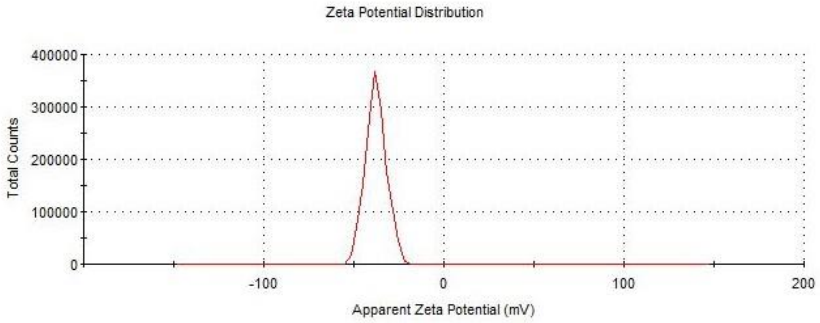

Figure S2: *Screenshot of Zeta Potential of GO dispersion after 15 minutes of sonication in a water bath. The concentration of GO detected is 50µg/mL in water.*

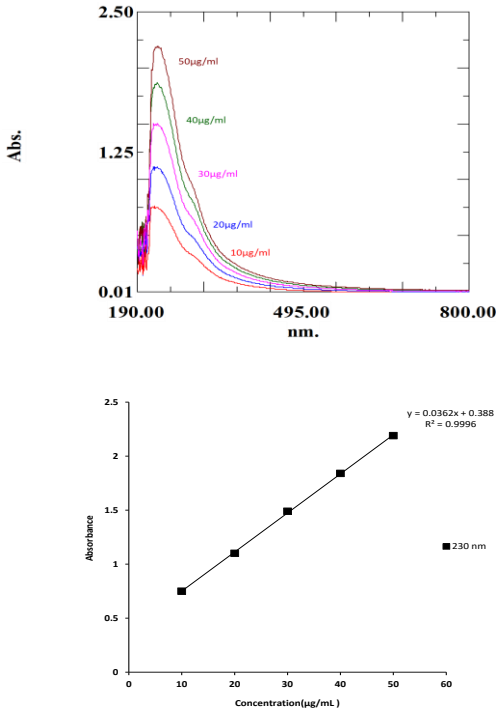

Figure S3: *The absorbance curve of different concentration of Graphene Oxide solution and the standard curve at 230nm.*